Available online at www.sciencedirect.com

ScienceDirect

Ceramics International 39 (2013) 9055–9061

CERAMICS INTERNATIONAL

www.elsevier.com/locate/ceramint

Preparation of dehydroxylated and delaminated talc: Meta-talc

Petr Ptáček*, Tomáš Opravil, František Šoukal, Jaromír Havlica, Jiří Másilko, Jaromír Wasserbauer

Brno University of Technology, Faculty of Chemistry, Center for Materials Research CZ.1.05/2.1.00/01.0012, Purkyňova 464/118, Brno, CZ-612 00, Czech Republic

Received 2 April 2013; accepted 29 April 2013
Available online 16 May 2013

Abstract

The roentgen-amorphous delaminated and dehydroxylated phase was prepared applying intensive milling procedure and subsequent thermal treatment of talc. Due to the similarity in properties and in thermal behavior of this material with roentgen-amorphous delaminated and dehydroxylated kaolinite phase, i.e. meta-kaolinite, the name meta-talc was suggested for this material. The properties and the behavior during thermal treatment were investigated using thermal analysis, x-ray diffraction analysis, infrared spectroscopy and scanning electron microscopy. The suggested procedure changes the activation energy of dehydroxylation, the behavior during thermal treatment and the phase composition of the product. The kinetics and thermodynamics of the thermal transition were evaluated using Kissinger equation and Eyering law.

Keywords: Talc; Meta-talc; Enstatite; Clay minerals; Heterogeneous kinetics

1. Introduction

Talc is a mineral of hydrous magnesium silicate with the composition given by formula $3MgO \cdot 4SiO_2 \cdot H_2O$ or $Mg_3Si_4O_{10}(OH)_2$. It is widely used due to its properties such as chemical inertness, softness, whiteness, high thermal conductivity, adsorption properties, etc. in numerous industrial applications, e.g. production of ceramics, as the filler for paper, paints, rubber and polymers [1–4]. Mineralogy classifies talc as the monoclinic magnesium-rich phyllosilicate from the group of talc and pyrophyllite ($Al_2Si_4O_{10}(OH)_2$). The structure of talc consists of tri-octahedral (brucite) sheets of magnesium octahedra (O) which are each interplayed between two sheets of silicon tetrahedra (T) forming so called T–O–T complex or 2:1 layer complex. The T–O–T sheets hold together by weak van der Waals forces [5].

The endothermic dehydroxylation of talc (Eq. (1)) takes place at 870–1050 °C resulting in the weight loss of about 4%. The recrystallization of the enstatite ($MgO \cdot SiO_2$) product phase is virtually immediate and accompanied by the separation of a silica-rich phase that recrystallizes to cristobalite under further heating [4].

$$3MgO{\cdot}4SiO_2{\cdot}H_2O \overset{T}{\Longrightarrow} 3MgO{\cdot}SiO_2 + SiO_2\ (\text{amorphous}) + H_2O\ (g) \quad (1)$$

The kinetics of the dehydroxylation of talc was investigated by Ward [6] who found that the reaction follows the first-order kinetics. The enthalpy of activation was found to be 423 ± 17 kJ mol^{-1}, and the entropy of activation was found to be 67 ± 17 J · (mol K)$^{-1}$.

The delamination and the loss of crystalinity caused by the tangential strain induced by the mills of different types was observed by many authors [1,7–10], but subsequent thermal treatment of the fully delaminated talc phase provides an option to prepare the delaminated and dehydroxylated roentgen-amorphous phase. This material (mechanicaly and thermally activated talc) can be analogical with delaminated and dehydroxylated roentgen-amorphous metakaoline termed as meta-talc. This work deals with the preparation procedure, properties and behavior during thermal treatment of meta-talc. The activation energy of endothermic dehydroxylation and exothermic transformation into enstatite and the frequency factor were calculated via Kissinger kinetics approach.

*Corresponding author. Tel.: +420 541 149 389; fax: +420 541 149 361.
E-mail address: ptacek@fch.vutbr.cz (P. Ptáček).

0272-8842/$ - see front matter © 2013 Elsevier Ltd and Techna Group S.r.l. All rights reserved.
http://dx.doi.org/10.1016/j.ceramint.2013.04.109

2. Experimental procedures

2.1. Sample, sample treatment and characterization

The sample of talc powder with the median of particle size of 5.9 μm (Particle size analyzer Helos, Sympates) was used in this work. The sample was milled by stainless steel vibratory mill for different time periods (0, 10, 20, 30, 60, 90 and 120 min) and the behavior of the material under thermal treatment was investigated. The samples which were mechanically treated for longer time periods were milled in 30 min intervals to avoid their heating to the temperatures higher than 60 °C.

The state of the sample after the treatment was characterized by the x-ray diffraction analysis (X'pert Empyrean, PANanalytical) using Cu(K_α) radiation at 40 kV and current 40 mA. The high temperature chamber HTK 16 (Anton Paar) was used to investigate high temperature transformations via HT-XRD analysis. The XRD pattern was collected with the step of 25 °C. The Fourier transform infrared spectroscopy (FT-IR) was applied with FT-IR analyzer Nicolet iS10 (Thermo Scientific) using KBr pellets technique. The sample was carefully weighted and mixed with dry KBr in the mass ratio 1:100 and the pellets weighing 120 mg each were hand pressed from the mixture using the force of 80 kN. The infrared spectrum was collected with the resolution of 8 cm^{-1} using 128 scans. The texture analyses of samples of kaolin treated at different time intervals were performed by means of scanning electron microscopy (SEM) using Field emission electron microscope Jeol JSM-7600F.

2.2. Kinetics and thermodynamics background

The non-isothermal kinetics experiments were performed with TG-DTA analyzer SDT Q600 (Thermal instruments). The sample of 30 mg was inserted into the platinum cup and heated with the heating rates (Θ) from 2 to 20 °C min^{-1} up to 1100 °C. The apparent activation energy (E_a) and the frequency factor (A) of investigated process were evaluated by the mechanism-free method based on the Kissinger kinetics approach [11]:

$$\ln\left[\frac{\Theta}{T_m^2}\right] = \ln\left[\frac{AR}{E_a}n(1-\alpha)^{n-1}\right] - \frac{E_a}{RT_m} = const. - \frac{E_a}{RT_m} \quad (2)$$

where Θ is the heating rate, n is the empirical reaction order (kinetic exponent), α is the conversion degree (fractional conversion) and R is the universal gas constant. The constant term is equal to ln (AR/E_a) for the first-order type and pseudo first-order type of reaction.

The crystallization mechanism was estimated from the shape of DTA peak. The peaks' parameters of TA curves enable to determine the value of kinetic exponent (n) which is related to the empirical order of reaction [11]. The exponent can be calculated from the equation [12,13]:

$$n = \frac{2.5RT_m^2}{w_{1/2}E_a} \quad (3)$$

where $w_{1/2}$ is the half-width (width at half high) of peak. The value of kinetic exponent is typical for various mechanisms of the investigated process [14].

The correlation between kinetic and thermodynamic parameters of the activated complex results from the combination of Arrhenius equation with Eyring or Wertera and Zenera laws related to the temperature dependence of the rate constant ($k(T)$) [15]:

$$k(T) = A\exp\left[-\frac{E_a}{RT}\right] = \frac{k_B T}{h}\exp\left[\frac{\Delta S\#}{R}\right] \exp\left[\frac{-\Delta H\#}{RT}\right] = \nu\exp\left[\frac{-\Delta G\#}{RT}\right] \quad (4)$$

where k_B, h and $\nu = k_B T/h$ are the Boltzmann constant, the Plank constant and the vibration frequency, respectively. The thermodynamic parameters of activated complex, including Gibbs energy (free enthalpy) ($\Delta \boldsymbol{G}^{\#}$), enthalpy ($\Delta \boldsymbol{H}^{\#}$) and entropy ($\Delta \boldsymbol{S}^{\#}$) of the process were calculated using Eyring equations [15–18]:

$$\Delta H\# = E_{a,\alpha} - RT_\alpha \quad (5)$$

$$\Delta S\# = R\left[\ln\left(\frac{hA_\alpha}{k_B T_\alpha}\right) - 1\right] \quad (6)$$

$$\Delta G\# = \Delta H\# - T_\alpha \Delta S\# \quad (7)$$

The thermodynamic parameters are often calculated using the peak temperature T_m so that the values $\Delta G^{\#}$, $\Delta H^{\#}$ and $\Delta S^{\#}$ are related to the highest rate of the process [18].

3. Results and discussion

The milling procedure leads to the gradual disappearing of crystalline structure of talc as was shown in Fig.1. The results of quantitative XRD Rietveld analysis indicate pure clay with the content of talc of 100%. The interlayer distance for applied talc was calculated from the structure refinement of XRD data to the length of 9.40 Å.

The sample is completely amorphous after 60 min of milling, but the time necessary for complete destruction of crystalline structure depends on the kind of mill and milling procedure as well. Therefore it is necessary to identify the structural parameter in order to characterize the state of material. The diffraction lines related to [001] planes vanish the fastest due to the layered structure of mineral while the features in [−111] direction are the most persistent [1,9].

In this work the Delamination and Amorphization Index (DAI) was derived from the structure of talc cell in order to evaluate the degree of delamination, i.e. destruction of layered structure of talc, and amorphization, i.e. the gradual disappearing of crystalline structure during milling procedure. The DAI index is defined as follows:

$$\mathrm{DAI} = \frac{I_{020}}{I_{004} + I_{-111} + I_{110}} \quad (8)$$

where I_{xyz} denotes the intensity of diffraction line according to Fig.1. The index value is close to one for untreated sample of well crystalline structure. The values higher than one are

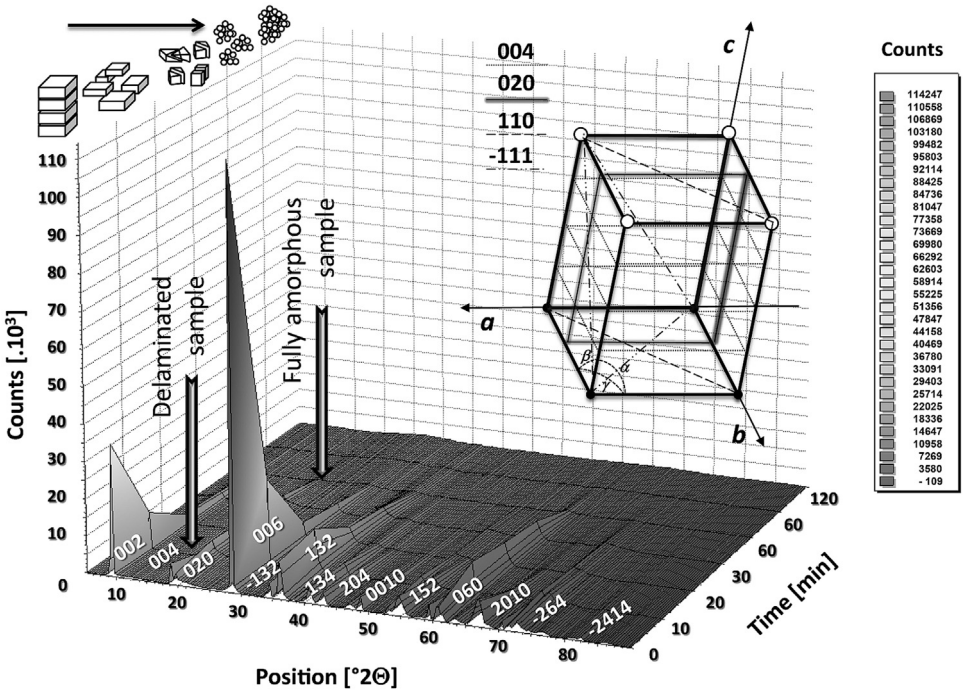

Fig. 1. The changes of XRD pattern with time of milling.

Table 1
The influence of time of treatment on the delamination and amorphization index.

Time [min]	0	10	20	30	60	90	120
DAI	1.04	0.83	0.79	0.47	0.22	DAI→0	
			DAI→0.8, the sample is fully delaminated.			Amorphous sample	

Table 2
The effect of milling procedure on the median of particle size and the specific surface of talc.

Treatment	[min]	0	10	20	30	60	90	120
SS	[$m^2\ g^{-1}$]	6.28	2.20	1.97	1.53	2.07	1.97	3.33
x_{50}	[μm]	5.87	1.97	3.82	2.62	5.11	14.45	1.15
m_p		8.62	1.94	1.22	1.10	1.22	0.93	1.02
m_a		—	19.44	19.13	11.16	10.27	9.95	9.72

reached in case that preferred orientation of lamellar talc particles takes place. The index decreases by gradual delamination of talc structure and the value close to 0.8 was assessed for fully delaminated sample. The diffraction line [004] disappears at the same time. The destruction of crystalline lattice leads to further decreasing of DAI to the limit value of zero for fully amorphous sample. The changes of DAI index during the treatment of talc are introduced in Table 1.

Table 2 and Fig. 2 introduce the changes in morphology, specific surface (SS), median of cumulative distribution function (x_{50}) of particle size and in mode of density distribution curve for primary particles (m_p) and aggregates (m_a) of talc during treatment.

Large clusters of talc sheets (a) are ground to the small plate-like particles (b) which are subjected to fast delamination (please refer to Fig. 1). Primary particles form aggregates bound into large spherical clusters by weak van der Walls interactions. The mode of particles size decreases in the initial stage of process (approximately first 20 min) only, nevertheless the mode of size of aggregates keeps decreasing till the end of amorphization (~60th minute of milling process) where only

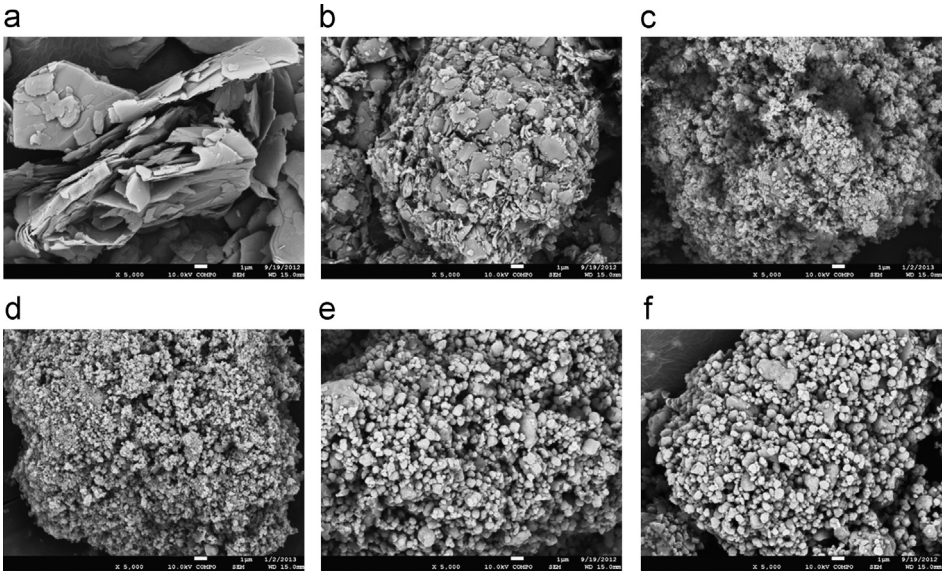

Fig. 2. SEM picture of talc mechanically treated for different time intervals.

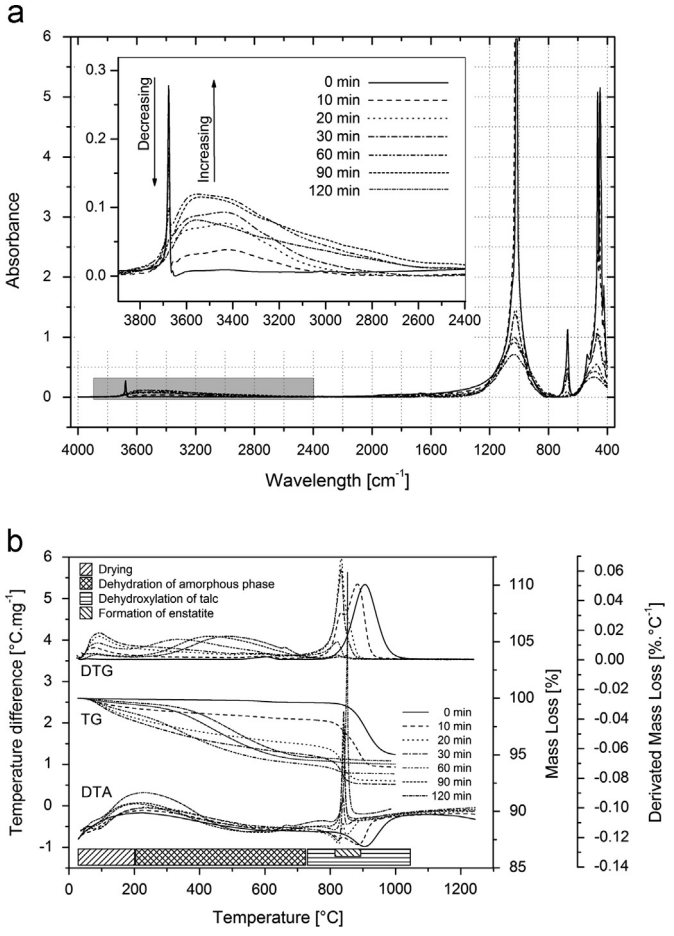

Fig. 3. Infrared spectrum of mechanically treated talc (a) and the results from thermal analysis (b).

irregular particles can be recognized (d). Further mechanical treatment does not cause the reduction of the size of particles and aggregates but hammers the sample to the side of mill.

The destruction of T–O–T structure of talc implies also from the results of infrared spectroscopy (Fig.3). The strain stress induced by milling procedure leads to the decrease of intensity and to broadening of spectral features. The destruction of brucite sheet is related to disappearing intensity of Mg–OH stretching (3678 cm^{-1}), deformation (669 cm^{-1}) band and Mg–O bond (535 cm^{-1}). The intensities of Si–O stretching (1018 cm^{-1}), Si–O–Mg stretching (449 cm^{-1}) and Si–O deformation (424 cm^{-1}) decrease as well. With the time of treatment, the intensity of stretching and the deformation bands of water which are located at 3553 cm^{-1} and 1650 cm^{-1} increase.

The TG-DTA plot of original sample shows endothermic dehydroxylation of talc at the temperature of 906 °C. The mass of sample decreases by 4.8 wt% during this process. The peak temperature increases with increasing time interval of mechanical treatment. The milling process shows opposite effect through the sharp exothermic peak of formation of enstatite phase at average temperature of 840 °C. The mechanical treatment also intensifies the effects related to the initial evaporation of water (drying) and dehydration of formed amorphous phase which take place in the temperature range from 300 to 650 °C.

The treatment also causes changes in the thermal behavior and the phase composition of product (Fig.4). Original talc (a) is transformed into orthorhombic enstatite from 850 to 1050 °C, while the mixture of enstatite and monoclinic clinoenstatite crystalizes from the amorphous sample (b).

The kinetics of dehydroxylation was evaluated using the temperature of DTG peak and plotting ln $[\Theta/T_p^2]$ vs. reciprocal temperature as the slope of Kissinger plot (Fig.5). The intercept with *y*-axis and the kinetic exponent calculated from Eq. (3) were used for the calculation of value of frequency factor from the Kissinger equation.

The overview of determined values of kinetic triplet and of thermodynamic data is given in Table 3. The influence of treatment on the kinetics of dehydroxylation implies from

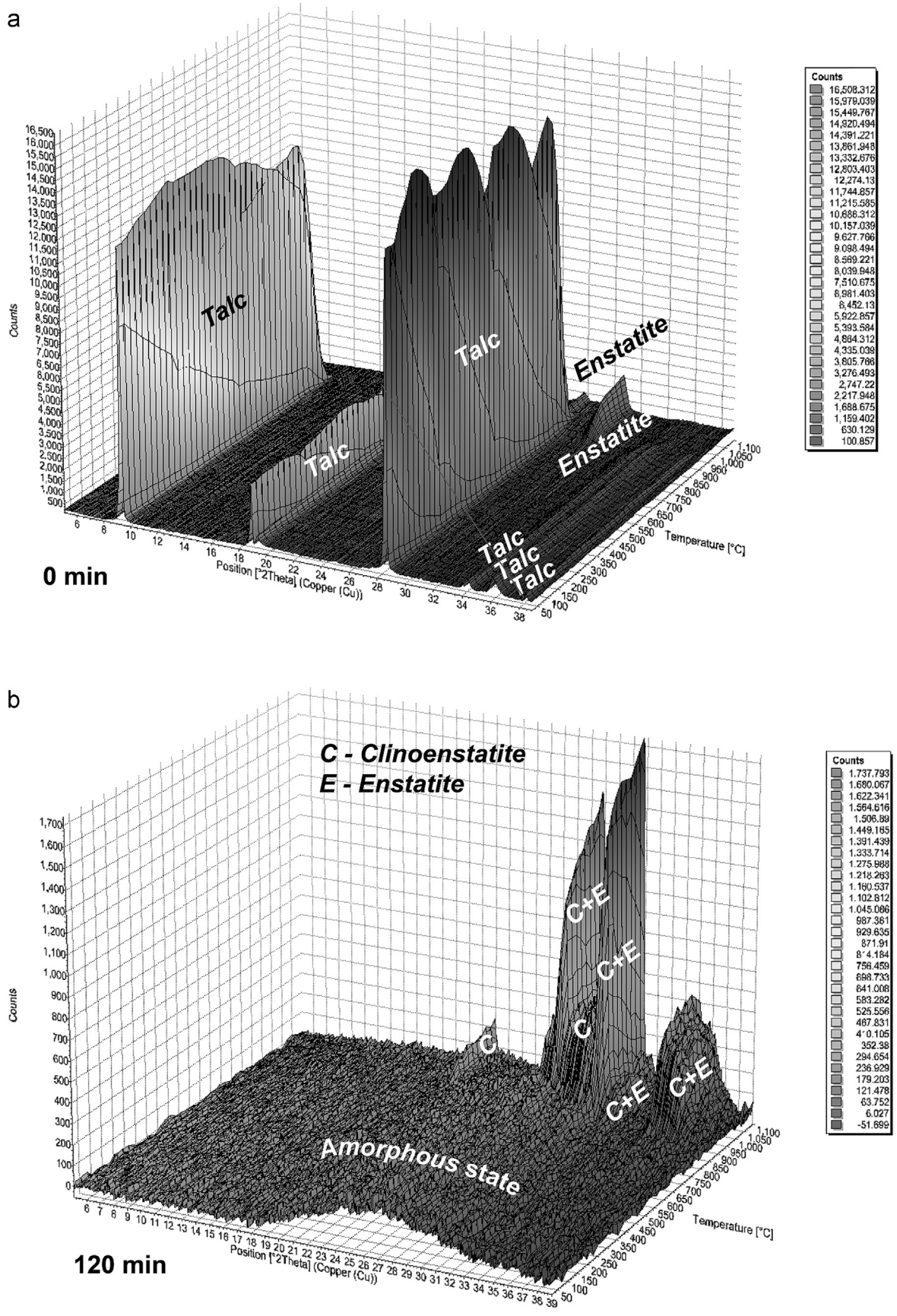

Fig. 4. HT-XRD analysis of original talc (a) and talc treated for 120 min (b).

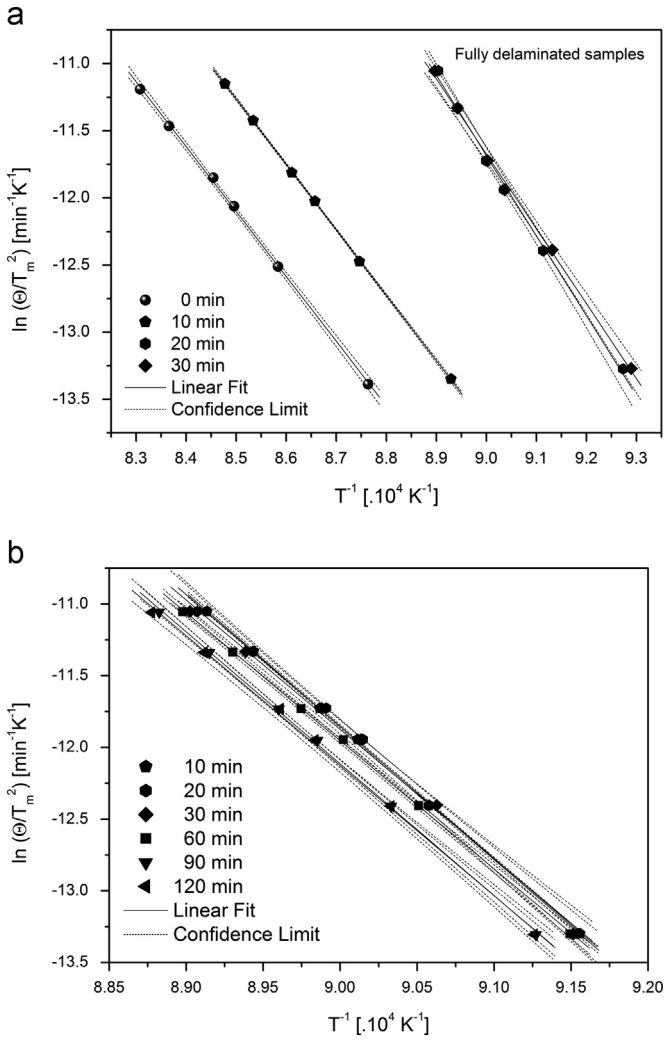

Fig. 5. The Kissinger plot of dehydroxylation of original sample of talc (a) and of crystallization of enstatite from treated sample (b).

these data while the crystallization of enstatite is not significantly affected.

The average value of apparent activation energy of dehydroxylation for untreated and fully delaminated sample increases from 404 ± 4 to 483 ± 11 kJ mol^{-1}, respectively. The assessed value of kinetic factor of dehydroxylation (1.1 ± 0.2) shows that the process is limited by the rate of growth of plate particles. The average apparent activation energy which relates to the crystallization of enstatite phase is 755 ± 9 kJ mol^{-1}. The value of kinetic factor is 2.8 ± 0.3. Therefore the crystallization of enstatite is driven by instantaneous nucleation of a new phase, i.e. the process limited by zero nucleation rate takes place.

4. Conclusion

The dehydroxylation of talc requires the apparent activation energy of 404 ± 4 kJ mol^{-1}. This value rises to 483 ± 11 kJ mol^{-1} for delaminated product. The average value of empirical reaction order of 1.1 ± 0.2 indicates the first order kinetic process. While the mechanism of dehydroxylation is not

Table 3
The effect of treatment on the kinetics of dehydroxylation.

Time of treatment [min]			0	10	20	30	60	90	120
Dehydroxylation of talc	E_a	[kJ mol^{-1}]	402[a]	405	489[b]	478	Peak of dehydroxylation cannot be recognized.		
	A	[s^{-1}]	$3.2 \cdot 10^{15}$	$2.8 \cdot 10^{16}$	$2.4 \cdot 10^{21}$	$4.6 \cdot 10^{20}$	The sample is in amorphous state.		
	n		1.0[a]	0.9	1.2	1.4			
	$G^{\#}$	[kJ mol^{-1}]	355	338	319	324			
	$H^{\#}$	[kJ mol^{-1}]	392	396	479	469			
	$S^{\#}$	[kJ mol^{-1} K^{-1}]	32	50	145	131			
Crystallization of enstatite	E_a	[kJ mol^{-1}]	The peak is not present	772	742	750	747	765	754
	A	[s^{-1}]		$9.1 \cdot 10^{33}$	$1.2 \cdot 10^{33}$	$2.8 \cdot 10^{33}$	$1.2 \cdot 10^{33}$	$7.1 \cdot 10^{33}$	$3.9 \cdot 10^{33}$
	n			2.3	3.2	2.4	2.7	2.9	3.0
	$G^{\#}$	[kJ mol^{-1}]		335	332	324	328	329	323
	$H^{\#}$	[kJ mol^{-1}]		763	733	741	738	756	744
	$S^{\#}$	[kJ mol^{-1} K^{-1}]		386	368	376	369	383	378

[a]The determined values of E_a and mechanism show good agreement with the literature [6].
[b]Sample is fully delaminated.

affected by the mechanical treatment, the behavior and the phase composition of sample during the thermal treatment is different form original talc. The mixture of orthorhombic enstatite and monoclinic clinoenstatite crystallizes from the amorphous phase at the temperatures higher than 800 °C. The E_a of the process was determined 755 ± 9 kJ mol^{-1}. The value of kinetic factor of 2.8 ± 0.3 indicates the instantaneous nucleation of new phase.

The fully delaminated and amorphized talc treated to the temperature lower than 800 °C remains roentgen-amorphous, hence amorphous delaminated as well as dehydroxylated phase can be prepared. This phase can be termed as meta-talc analogically to the relationship between kaolinite and meta-kaolinite.

Acknowledgments

This work was supported by the Project of Ministry of Education, Youth and Sports of the Czech Republic No. CZ.1.05/2.1.00/01.0012 "Centre for Materials Research at FCH BUT" supported by Operational Program Research and Development for Innovations; and the project of Czech Science Foundation (GACR) No. P104/12/0913 "Activation of Silicates and Slags as a Carbonation Feedstock for CO_2 Mineral Storage".

References

[1] F. Dellisanti, G. Valdrè, M. Mondonico, Changes of the main physical and technological properties of talc due to mechanical strain, Applied Clay Science 42 (2009) 398–404.
[2] T.K. Mukhopadhyay, M. Das, S. Ghosh, S. Chakrabarti, S. Ghatak, Microstructure and thermo mechanical properties of a talc doped stoneware composition containing illitic clay, Ceramics International 29 (2003) 587–597.
[3] L.A. Pérez-Maqueda, A. Duran, J.L. Pérez-Rodríguez, Preparation of submicron talc particles by sonication, Applied Clay Science 28 (2005) 245–255.
[4] K.J.D. MacKenzie, R.H. Meinhold, The thermal reactions of talc studied by ^{29}Si and ^{25}Mg MAS NMR, Thermochimica Acta 244 (1994) 195–203.
[5] E. Burdukova, M. Becker, D.J. Bradshaw, J.S. Laskowski, Presence of negative charge on the basal planes of New York talc, Journal of Colloid and Interface Science 315 (2007) 337–342.
[6] J.R. Ward, Kinetics of talc dehydroxylation, Thermochimica Acta 13 (1975) 7–14.
[7] M.-P. Flament, P. Leterme, M. Bizi, G. Baudet, A. Gayota, Study of talcs as antisticking agents in the production of tablets, European Journal of Pharmaceutical Sciences 17 (2002) 239–245.
[8] E.F. Aglietti, J.M.P. Lopez, Physicochemical and thermal properties of mechanochemically activated talc, Materials Research Bulletin 27 (1992) 1205–1216.
[9] H. Yang, Ch. Du, Y. Hu, S. Jin, W. Yang, A. Tang, E.G. Avvakumov, Preparation of porous material from talc by mechanochemical treatment and subsequent leaching, Applied Clay Science 31 (2006) 290–297.
[10] Junya Kano, Miyuki Miyazaki, Fumio Saito, Ball mill simulation and powder characteristics of ground talc in various types of mill, Advanced Powder Technology 11 (2000) 333–342.
[11] H.E. Kissinger, Reaction kinetics in differential thermal analysis, Analytical Chemistry 29 (1957) 1702–1706.
[12] J.A. Augis, J.D. Bennett, Calculation of Avrami parameters for heterogeneous solid-state reactions using a modification of Kissinger method, Journal of Thermal Analysis 13 (1978) 283–292.
[13] C.S. Ray, Q. Yang, W.-H. Huang, D.E. Day, Journal of the American Ceramic Society 79 (1996) 3155.
[14] J. Málek, The applicability of Johnson–Mehl–Avrami model in the thermal analysis of the crystallization kinetics of glasses, Thermochimica acta 267 (1995) 61–73.
[15] J. Straszko, M. Olszak-Humienik, J. Možejko, Kinetics of thermal decomposition of ZnSO4 · 7H2O, Thermochimica Acta 292 (1997) 145–150.
[16] J. Straszko, M.O. Humienik, J. Mozejko, Thermochimica Acta 292 (1997) 145.
[17] S.M. Pourmortazavi, I. Kohsari, M.B. Teimouri, S.S. Hajimirsadeghi, Thermal behaviour kinetic study of dihydroglyoxime and dichloroglyoxime, Materials Letters 61 (2007) 4670–4673.
[18] L. Vlaev, N. Nedelchev, K. Gyurova, M. Zagorcheva, A comparative study of non-isothermal kinetics of decomposition of calcium oxalate monohydrate, Journal of Analytical and Applied Pyrolysis 81 (2008) 253–262.